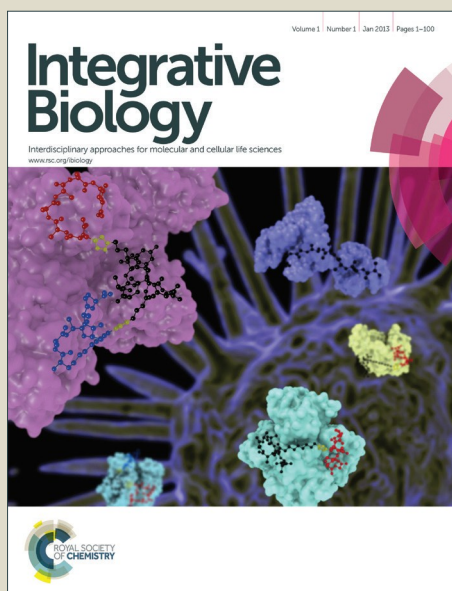


Integrative Biology

Accepted Manuscript



This is an *Accepted Manuscript*, which has been through the Royal Society of Chemistry peer review process and has been accepted for publication.

Accepted Manuscripts are published online shortly after acceptance, before technical editing, formatting and proof reading. Using this free service, authors can make their results available to the community, in citable form, before we publish the edited article. We will replace this *Accepted Manuscript* with the edited and formatted *Advance Article* as soon as it is available.

You can find more information about *Accepted Manuscripts* in the [Information for Authors](#).

Please note that technical editing may introduce minor changes to the text and/or graphics, which may alter content. The journal's standard [Terms & Conditions](#) and the [Ethical guidelines](#) still apply. In no event shall the Royal Society of Chemistry be held responsible for any errors or omissions in this *Accepted Manuscript* or any consequences arising from the use of any information it contains.

Insight box

Our work provides a novel view regarding the mechanobiology of adipogenesis, with correlation between cell morphology and cell-gel mechanics. Concurrently monitoring cell morphology and the magnitude and patterns of forces applied by cells to a soft gel, using traction force microscopy, we were able to show an important phenomenon: The proportionality of the total traction force and the cell contact area is preserved before and during differentiation up to 14 days in culture. The constancy of this ratio points to a specific 'stress output' which characterizes the mechanical interaction of differentiating adipocytes with their substrate. The work provides new insights into the progression of differentiation of adipocytes.

Ratio of total traction force to projected cell area is preserved in differentiating adipocytes

Cite this: DOI: 10.1039/x0xx00000x

Shada Abuhattum^a, Amit Gefen^b and Daphne Weihs^a

Received 00th February 2015,
Accepted 00th January 2015

DOI: 10.1039/x0xx00000x

www.rsc.org/

During obesity development, preadipocytes proliferate and differentiate into new mature adipocytes, to increase the storage capacity of triglycerides. The morphology of the cells changes during differentiation from an elongated spindle-shape preadipocyte into a rounded, differentiated adipocyte. That change allows efficient packing of spheroidal lipid droplets in the cells, also reducing their ability to proliferate and migrate. The change in preadipocyte morphology is well known. However, little is known about the dynamic mechanical interactions of the cells with their microenvironment, and specifically the forces applied by the cells during and after differentiation. In this study, we evaluated changes in the morphology concurrently with the magnitude and location of forces applied by the cells onto a compliant gel-substrate. We found that the elongated preadipocytes applied forces concentrated at the poles of the cell, yet during differentiation the forces become more uniformly distributed around the cell and mostly at its perimeter. Furthermore, we observed that the total traction force per cell area is preserved, remaining essentially unchanged between preadipocytes and differentiated cells 3-14 days post-differentiation. At differentiation times longer than 8 days we also observed an increasing subset of cells that indent the gels, as opposed to merely applying horizontal traction forces. Our work provides insights into the dynamic mechanobiology of the adipogenesis process.

Introduction

Obesity is widely recognized as a major public health problem in developing and developed countries, and is associated with a number of serious chronic diseases including hyperlipidemia, hypertension, type II diabetes, various cancers, and coronary atherosclerotic heart disease.^{1, 2} The prevalence of obesity is escalating worldwide as 500 million individuals aged over 20, and 40 million children were classified with obesity in 2008 and 2010, respectively.^{3, 4} Those statistics account for approximately \$150 billion in annual medical costs.^{5, 6} Thus, it is highly important to identify the causes of obesity at the cell-level, which can reveal targets for treatment and treatment strategies beyond conventional nutritional or exercise recommendations.

The development of obesity is characterized by two processes: using existing adipocytes (fat cells) or in development of new adipocytes – adipogenesis. In existing adipocytes, lipid droplets enlarge to increase the storage capacity of triglycerides.⁷ In parallel, new preadipocytes may be recruited from

mesenchymal stem cells, and differentiate into adipocytes. Conventional thinking relates adipogenesis to the excess of energy intake. Thus, conservative treatments for obesity are aimed at decreasing the body mass by physical exercise together with reduction of the calorie intake. Other than intake and consumption of calories, body energetics are also influenced by the individual metabolic rates in tissues, the health status, genetics and other biological and biochemical factors. However, recent studies suggest that obesity development is highly affected by the adipocytes' mechanical environment.^{7, 8} Specifically, when preadipocytes are mechanically stretched either statically or cyclically, and for an extended period of time, their morphology changes and the adipogenesis process is, respectively, accelerated⁸ or inhibited.⁹ These findings emphasize the importance of the mechanical interactions of developing adipocytes with their environment. The mechanical interactions of living cells with their environment may be evaluated using traction force microscopy. Here, traction forces applied by cells are determined through the deformation induced to 2-dimensional or 3-dimensional compliant gels.^{10, 11} The traction forces are calculated by correlating the force-induced gel deformation with the measured gel stiffness and its Poisson's ratio. This approach

^a Faculty of Biomedical Engineering, Technion-Israel Institute of Technology, Haifa 3200003, Israel

^b Department of Biomedical Engineering, Tel Aviv University, Tel Aviv 69978, Israel

has been used, for example, to evaluate traction forces associated with fibroblast migration,¹² tumour cell migration,¹³ to measure contractility of vascular smooth muscle cells,¹⁴ and even modified to evaluate normal forces applied by cancer cells.^{15, 16}

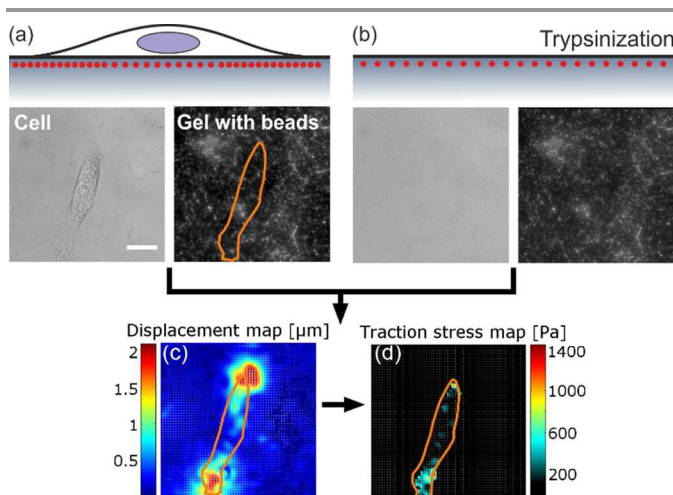


Fig. 1 Experimental procedure for traction force microscopy experiments. (a) Image of cells seeded for 24 hours on polyacrylamide gel with fluorescent beads at its surface. The orange line is the cell boundary. Schematic shows adhered cell applying horizontal traction force and pulling the gel towards its centre, moving the beads closer; (b) Cells are removed from the gel (using trypsin) to obtain the reference state with a relaxed gel. The schematic shows that gel relaxes and beads return to their original spacing; (c) Bead displacements between the deformed and relaxed gel provide the displacement map; (d) Traction stress map is calculated from the strain map. Scale bar 20 μm , colour bars provide displacement and stress map scaling.

Many studies have been focused on the effects of stiffness or degradability of the matrix on the lineage commitment and fate of stem cells, with special focus on naïve mesenchymal stem cells (MSCs). On non-degradable 2D substrates it is the stiffness and elasticity of the substrate that strongly influences the eventual fate of MSCs.¹⁷ In contrast, if the matrix is degradable (and 3D), cell fate is less dependent on the matrix stiffness, and depends more on the traction forces that cells develop following matrix degradation.¹⁸ A point of interest has been identifying early indications of the differentiation process, before the phenotype is evident and identifiable through a typical cell morphology. Heterogeneities in 2D traction forces were observed in cells less than 7 days following differentiation, where at longer times, differences correlating to MSC commitment (osteogenic or adipocytic) became apparent.¹⁹ During the first 7 days post differentiation, MSCs exhibited reduction in cell elasticity and membrane compliance²⁰ concurrently with an increase followed by a decrease in traction force per area applied by the cells to a 2D substrate.¹⁹ A direct correlation has been observed between the traction forces applied by differentiating MSCs and the cell spreading area, linked to the amount of focal adhesions utilized by the cells.¹⁹ Focal adhesions are connected to intracellular actin, and accordingly, in the presence of adipogenic differentiation factors at early stages of differentiation (7 days), actin-network stiffening was observed concurrently with

increased traction stresses applied to the substrate²¹; increased stress was related to an increase in contractility genes but not an increase in focal adhesions. In our present work, we use preadipocyte cells already committed to the adipose lineage (3T3-L1, ATCC®), and thus the time-scales of differentiation and onset of synthesis and accumulation of triglycerides may differ with respect to differentiation of MSCs. The preadipocytes used in our study are also sensitive to lipogenic and lipolytic hormones including insulin; we use insulin in the culture media to accelerate adipogenesis. Further, we present results, for the first time in the literature, which extend beyond 7 days in differentiation media.

Here, our objective was to evaluate changes occurring in the cell-substrate mechanical interactions as adipocytes differentiate. Specifically, we measured the forces applied by cells starting at the preadipocyte stage and progressing to maturation and adipogenesis, up to 14 days post induction of differentiation. Mechanotransduction was recently shown to be strongly involved in adipogenesis.^{7, 8, 22, 23} The present study covers an additional critical mechanobiological aspect that has not been studied before: how morphology, forces and patterns of force application relate and change during different stages of adipocyte differentiation. Better understanding of mechanotransduction in adipocytes will open new research pathways towards controlling or perhaps even curing obesity. We observed that regardless of the differentiation time, preadipocytes and differentiating adipocytes exhibit an essentially unchanging ratio of the total applied traction force to the cell area in contact with the substrate. The preadipocytes applied forces that were localized specifically at the poles of the spindle-structured cells. In contrast, differentiating adipocytes were rounded, and applied forces more uniformly around their perimeter; adipocyte forces were focussed mostly at the cell boundaries and less under the cell centres.

Results and discussion

We have monitored changes in cell morphology as well as magnitudes and spatial distributions of forces applied by the adipocytes before and throughout different times in the differentiation process. Single cells were cultured on collagen-coated polyacrylamide gels (Young's modulus, $E=2440 \pm 40$ Pa) containing 200 nm fluorescence beads at their surface. The stiffness that we have chosen is in the mid-range of stiffness measured for human and animal abdominal and subcutaneous fat, the range of 0.3-3 kPa.^{24, 25} Following their differentiation period in plates, cells were cultured on the gels for 24 hours prior to any traction force measurements, to allow full adherence. Cells were seeded so that they were far enough apart so that no mechanical interactions between them are expected.²⁶ Fig. 1 provides a schematic of the experimental procedure. Following cell adherence, two images were captured: cell images using differential interference contrast (DIC) and an image of the fluorescence beads at the gel surface (Fig. 1a). To obtain the absolute value of the applied force, the reference state was a gel with no cells, and thus no applied force; cells

were removed with trypsin (Fig. 1b). The forces applied by each cell on the polyacrylamide gel was calculated using constrained traction-force microscopy,^{10, 11} where bead-displacements in the gel (Fig. 1c) are assumed to result only from traction forces applied by the cell, i.e. within the cell boundaries (Fig. 1d). The cell boundaries were marked manually using the DIC image of the cell, and the traction stress map was calculated in a specialized MATLAB module.

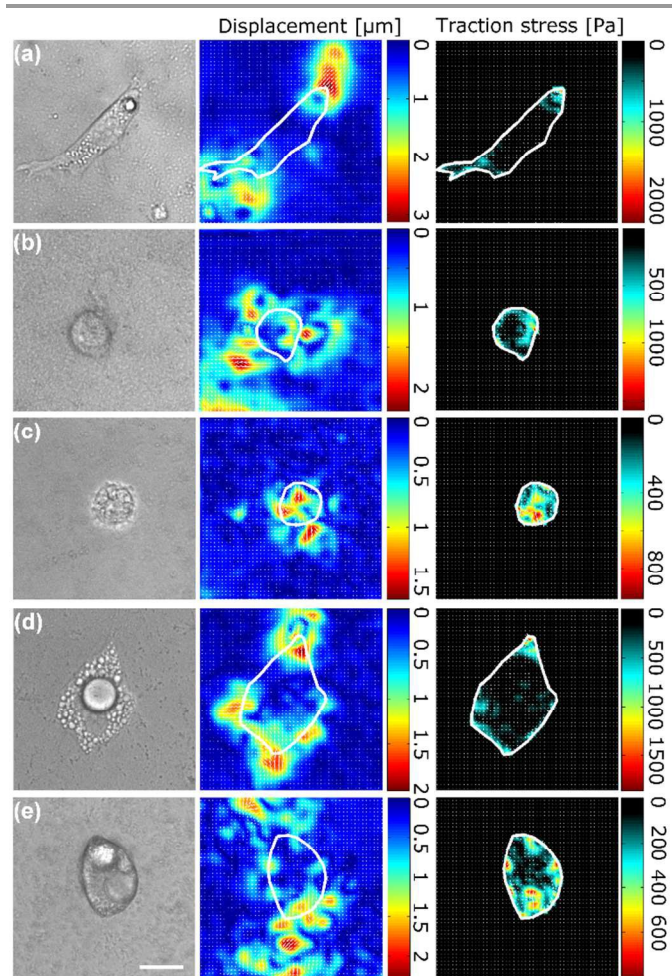


Fig. 2 Cells on gels exhibit changes in force magnitude and application locations following differentiation. By column: on left, representative cell morphologies; in middle column, displacement fields occurring in the gel with the cell perimeter marked in white; in right column, constrained traction stress fields. Forces are applied only where cells are present, yet continuous gels are deformed throughout. (a) In preadipocytes forces were concentrated at the cell poles. In contrast, cells after differentiation for (b) 3 days, (c) 8 days, (d) 11 days, and (e) 14 days were rounded and forces were more uniformly distributed along the cell peripheries. Scale bar is 20 μm for all panels, colour bars vary for each panel.

Fig. 2 shows the time dependent changes in the cell morphology and applied force following differentiation. The preadipocyte cells, which are fibroblast-like, exhibited spindle morphology (Fig. 2a) with traction stresses applied primarily at the cell poles, as is typical for adhered fibroblasts.¹⁰

Following differentiation, cells become more rounded in morphology (Fig. 2b-e) and apply forces in inherently different spatial configurations and magnitudes. At 8 days post induction

of differentiation and at longer times, cells exhibited identifiable lipid droplets that could be demonstrated by fixed-cell Oil Red O staining (under phase contrast microscopy) as well as by live-cell Nile Red (by fluorescent staining).²² The more uniform pattern of force application at the perimeters of the differentiating adipocytes likely facilitates anchoring of these non-migratory, rounded cells to the substrate. The location of applied forces is likely affected by the structural changes occurring in the differentiating cells. Specifically, as the cells become round and lipid droplets form, the intracellular structure, and in particular the structure and location of the cytoskeleton of the cells changes,²⁷ which affects how cells adhere and apply force.

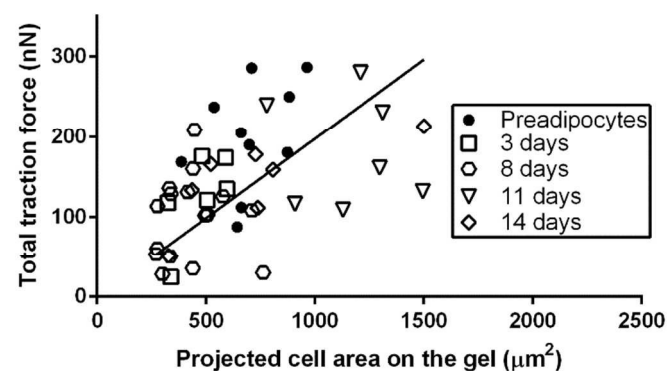


Fig. 3 The total traction force changes proportionately with the projected cell area for preadipocytes (full symbols) and adipocytes (empty symbols). The line provides a guide to the eye with a slope of 0.2 kPa (i.e. $\text{nN}/\mu\text{m}^2$).

We observed a wide distribution of areas and forces applied by the cells, however, the same ratio exists between the total traction force and the projected cell area at all times following initiation of differentiation as well as preadipocytes (Fig. 3). The total force²⁸⁻³⁰ is the sum of the magnitudes of the traction stress vectors (T , see Fig. 2) over the entire area of the cell (A), $F_{\text{total}} = \iint |\vec{T}(\vec{r})| dA$; it is typically considered as the force applied at all focal adhesions, or the force production (i.e. mechanical energy output) of the cell. Constant traction force per cell area had previously been observed in MSCs cultured within (non-differentiating) growth media,¹⁹ but not at the onset and progression of differentiation as noted here. In contrast, in naïve MSCs, up to 7 days into the differentiation process, the traction force was linear with the focal adhesion area (not cell area) and independent of substrate rigidity.¹⁹

The slope of the traction-applying cells is approximately 0.2 kPa (Fig. 3). It is interesting to note that the shear modulus of the gel is 0.8 kPa (as measured by rheometry), which is the relevant gel stiffness measure that counteracts the lateral forces applied by the cells. Concurrently, the shear modulus of the cytoplasm of adhered adipocytes is 0.26 kPa.²³ The fact that all these measures are on the same order of magnitude, likely infers structural stiffness continuity at the cell-gel interface, where the cells adapt to their mechanical environment (which in the literature, is often being referred to as the ‘mechanical homeostasis’ of cells).

We have observed that a subset of the differentiated cells (at 11 days post-differentiation and beyond) exhibit a different strategy for adhesion, which results in gel indentations, likely inferring normal force application^{15, 16}; those cells were not included in Fig. 3. With progression of differentiation, an increasing number of cells indented the gels and did not only apply horizontal traction forces (Fig. 4a). The reasoning for the more mature differentiated cells to rely more on adhesion strategies inducing gel indentation as opposed to (only) horizontal traction forces requires further extensive research. One explanation that can immediately be ruled out, however, is that the increasing weight of the cells as they differentiate and become larger causes the gels to bend. To show this, we have calculated the force ($F=mg$) that would be applied to a gel by the cell weight (mg). We assume a spherical cell, 3.8×10^{-8} mL (average of the measured cells at 14 days) and cell density of water (1 g/mL); differentiated cells include a large volume of triglycerides with lower density, hence this is an overestimation. We disregard buoyancy forces, thereby increasing the weight effects. Using a Hertz model of spherical contact results in indentation depth of 1.2×10^{-16} μm , which is 16-17 orders of magnitude smaller than the measured indentation depths shown in Fig. 4b.

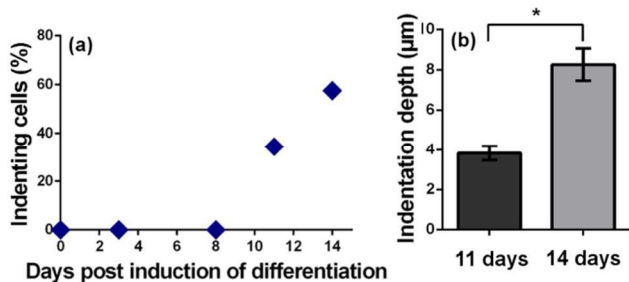


Fig. 4 A population of cells, beyond 8 days post induction of differentiation exhibit (normal force) induced indentations. (a) An increasing percent of cells indent the gels at long differentiation times. (b) The indentation depth attained by the indenting cells increases with the differentiation time. Bars are standard errors and values are significantly different ($p=0.0001$).

Experimental

Cell Culture

Mouse embryonic 3T3-L1 preadipocytes (American Type Culture Collection no. CL-173) were cultured in growth medium consisting of high-glucose (4.5 mg/mL) Dulbecco's modified Eagle's medium (DMEM, Gibco, Carlsbad, CA), supplemented with 10% fetal bovine serum (Hyclone Thermo Fisher Scientific, Waltham, MA), 1% each of L-glutamine and sodium pyruvate (Biological Industries, Kibutz Beit Haemek, Israel), and 0.1% penicillin-streptomycin (Sigma). Cells were cultured and maintained in a humidified incubator at 37°C, 5% CO₂ and were used at passages 10-20 from ATCC stock. When cultures reached 90% confluence, differentiation was induced by changing the growth medium to differentiation medium consisting of the growth medium supplemented with 3.15 $\mu\text{g/mL}$ insulin (Sigma), 1 μM dexamethasone (Sigma) and 2

μM 3-isobutyl-1-methylxanthine (Sigma). Three days after differentiation was first induced, the differentiation medium was replaced with supporting medium consisting of growth medium supplemented with 3.15 $\mu\text{g/mL}$ insulin only. The supporting medium was then changed every 2-3 days during the period of experiments.²²

Preparing Gels

Polyacrylamide gels were prepared according to an established protocol.^{10, 31} The surface of a glass cover slip, 30 mm diameter, #5 thickness (Menzel, Germany), was first coated with hydroxyl groups using 0.1 M NaOH, and then activated using 3-aminopropyltrimethoxysilan (both Sigma, St Louis, MO), then 2 μm diameter green fluorescent beads (Molecular Probes, Invitrogen Life Technologies, Carlsbad, CA) were adhered to the glass; their fixed position is used for de-drifting the images following small shifts with time. After 24 hours the glasses were activated with glutaraldehyde. Gels were prepared on ice and solutions were kept at 4°C. The gels were composed of 34 μL of 40 vol% acrylamide and 3.8 μL of 2 vol% BIS acrylamide (both from Bio-Rad, Israel) and 203 μL of distilled water, producing gels with Young's modulus of 2440 ± 40 Pa. Gelation was induced with 1:200 vol. ammonium persulphate (APS) as initiator and 1:500 vol. of Tetramethylethylenediamine (TEMED) as a catalyst (both from Sigma, St Louis, MO). The gel was generated on the glass cover slip using a plastic frames (Gene Frame, 25 μL , 10 \times 10 mm, ABgene Thermo-Scientific, Waltham, MA). Fluorescent, carboxyl-coated polystyrene particles, 200 nm in diameter (Molecular Probes, Invitrogen Life Technologies, Carlsbad, CA) were added to gels and localized to the gel surface by performing polymerization (gelation) at 2°C while centrifuging for 30 min at 300 g to bring particles to the gel surface.^{31, 32} After the polymerization the gels were rinsed with HEPES pH 8.5 (Sigma, St Louis, MO) and kept in phosphate buffered saline. Finally, the surface of the gel was activated with Sulfo-SANPAH (Pierce, Thermo Scientific, Waltham, MA) and coated with collagen (Rat tail type 1, Sigma, St Louis, MO). Glass cover slips were placed in a custom made 6-well plate and kept at 4°C until use.

Gel Stiffness

The Young's modulus of the gels was determined using a TA Instruments AR-G2 rheometer (New Castle, Delaware). Gels were prepared on the rheometer plate and the shear modulus was measured using a 2 cm diameter parallel plate fixture. Time sweep experiments were run during and following gelation (oscillatory strain of 0.5% and angular frequency of 3.14 rad/s) to determine the shear modulus, G^* . The Young's modulus, E , was then obtained using the following relation: $E=2|G^*|(1+\nu)$ where $\nu=0.49$ is the polyacrylamide gel Poisson's ratio.

Cell seeding and image acquisition

Cells were seeded on gels within their culture media (50,000 cells/2 ml) and were incubated in a humidified incubator at

37°C, 5% CO₂ for 1 day of cell incubation to facilitate attachment to the gels. Imaging was done with an automated Olympus IX81 inverted, epifluorescence microscope, using a 60x/0.7NA differential interference contrast (DIC, Nomarsky Optics) air-immersion, long working-distance objective lens. Images were taken using an XR Mega-10AWCL camera (Stanford Photonics Inc., Palo Alto, CA), at a final magnification of 107.8 nm/pixel.

Several single cells were imaged, each in a separate field of view; as cells are several widths apart, we do not expect mechanical interactions between them.²⁶ At each time-point and each field of view, three images were collected: DIC image of the cells on the gel, fluorescence image of the 200-nm diameter particles embedded at the gel surface, and a fluorescence image of the 2 μm diameter particles glued to the glass cover slip. After imaging the cells and the gel, the cells were removed using trypsin (Solution C EDTA 0.02%, Biological Industries, Kibutz Beit Haemek, Israel), and images of the same field of view without the cell were obtained.

Traction force microscopy data analysis

Images of beads at the gel surface and on the glass cover slip, respectively, provide a measure of the cell-induced deformation in the gel and allow us to correct for any local drift in the system. In addition, using the cell images, we are able to determine the exact location of the cells and constrain the cell-applied stresses to that area. Images were analyzed using a custom-designed module in MATLAB 2012b (The MathWorks, Natick, MA), kindly provided by Ramaswamy Krishnan, at Harvard.¹¹ In short, images of particles at the gel surface provided the deformation field through comparison of locations of the beads, using a sliding window of 32x32 pixels, on images with and without cells on the gel; this provides the displacement maps. Using the displacement field, we then calculated the traction forces constrained to within the cell boundaries, which were manually marked using custom MATLAB based codes. That is, outside the cell boundaries the stresses are brought to zero, using an iterative Fourier transform calculation procedure.¹¹

Indentation depth determination

We also use the particles at the gel surface as a measure for the indentation of the cells into the gel, as the gel surface is displaced to a lower optical focal plane.^{15, 16} When cells indent, we collect 3 images: a differential interference contrast (DIC) cell image, a fluorescence image of particles at the gel surface, and a fluorescence image of particles at the lowest indentation depth – the lowest focal depth where particles are observed. The focal depths corresponding to each image are obtained accurately through the microscope's electromechanical focus-step motor; the step motor resolution is 10 nm. The indentation depth is then calculated as the difference in focal depths between the two fluorescence images. Cells are considered as “indenting” when the depth exceeds 1 μm, which ensures that the indentations do not result from gel buckling due to traction forces only.^{15, 16}

Conclusion

In this work, we have evaluated the changes in morphology and forces applied by adipocytes to a compliant substrate before and during differentiation, up to 14-days. Concurrently monitoring cell morphology and the magnitudes and patterns of forces applied by cells to a soft gel using traction force microscopy and indentation depth measurements, we were able to show several important phenomena. Preadipocyte cells are initially elongated and spindle-like in morphology, applying forces at their poles. They then become rounded as they mature, and apply more uniformly distributed forces, mostly focused along the cell perimeters. At times longer than 8-days post induction of differentiation, an increasing number of cells also indent the gel. We specifically note the preservation of the proportionality of the total traction force and the cell contact area before and during differentiation (Fig. 3). The constancy of this ratio points to a specific ‘stress output’ that the adipocytes generate upon the gel, by applying forces at the cell-gel contact area through focal adhesions that are connected to the intracellular actomyosin network. Much like in a mechanical motor, where the power output results from the specifics of the design and interactions between components, the stress output of differentiating adipocytes appears to correlate (as reported for other cell types) between traction forces, the cell area and number of focal adhesions.

Acknowledgements

The work was partially funded by the Montreal and the Arcie Micay Biomedical Research Funds.

Notes and references

1. D. Goldstein, T. Elhanan, M. Aronovitch and D. Weihs, *Soft Matter*, 2013, 9, 7167-7173.
2. X. Ba, M. Rafailovich, Y. Z. Meng, N. Pernodet, S. Wirick, H. Furedi-Milhofer, Y. X. Qin and E. DiMasi, *J. Struct. Biol.*, 2010, 170, 83-92.
3. X. Yao, R. Peng and J. Ding, *Adv. Mater.*, 2013, 25, 5257-5286.
4. S. Bose, M. Roy and A. Bandyopadhyay, *Trends Biotechnol.*, 2012, 30, 546-554.
5. A. Stekelenburg, D. Gawlitza, D. L. Bader and C. W. Oomens, *Arch. Phys. Med. Rehabil.*, 2008, 89, 1410-1413.
6. P. Poirier, T. D. Giles, G. A. Bray, Y. Hong, J. S. Stern, F. X. Pi-Sunyer and R. H. Eckel, *Arterioscler. Thromb. Vasc. Biol.*, 2006, 26, 968-976.
7. N. Shoham and A. Gefen, *J. Biomech.*, 2012, 45, 1-8.
8. N. Shoham, R. Gottlieb, O. Sharabani-Yosef, U. Zaretsky, D. Benayahu and A. Gefen, *Am J Physiol-Cell Ph*, 2012, 302, C429-C441.
9. Y. Tanabe, M. Koga, M. Saito, Y. Matsunaga and K. Nakayama, *J. Cell Sci.*, 2004, 117, 3605-3614.
10. M. Dembo and Y. L. Wang, *Biophys. J.*, 1999, 76, 2307-2316.
11. J. P. Butler, I. M. Tolic-Norrelykke, B. Fabry and J. J. Fredberg, *Am J Physiol-Cell Ph*, 2002, 282, C595-C605.
12. S. Munevar, Y. L. Wang and M. Dembo, *Biophys. J.*, 2001, 80, 1744-1757.
13. C. T. Mierke, D. Rosel, B. Fabry and J. Brabek, *Eur. J. Cell Biol.*, 2008, 87, 669-676.
14. G. J. Ye, Y. Aratyn-Schaus, A. P. Nesmith, F. S. Pasqualini, P. W. Alford and K. K. Parker, *Integr. Biol.*, 2014, 6, 152-163.

ARTICLE

15. R. Kristal-Muscal, L. Dvir and D. Weihs, *New J Phys*, 2013, 15, 035022.
16. L. Dvir, R. Nissim, M. B. Alvarez-Elizondo and D. Weihs, *New J Phys*, 2015, 17, 043010.
17. A. J. Engler, S. Sen, H. L. Sweeney and D. E. Discher, *Cell*, 2006, 126, 677-689.
18. S. Khetan, M. Guvendiren, W. R. Legant, D. M. Cohen, C. S. Chen and J. A. Burdick, *Nat. Mater.*, 2013, 12, 458-465.
19. J. Fu, Y. K. Wang, M. T. Yang, R. A. Desai, X. Yu, Z. Liu and C. S. Chen, *Nat. Methods*, 2010, 7, 733-736.
20. I. Titushkin and M. Cho, *Biophysical journal*, 2007, 93, 3693-3702.
21. K. M. McAndrews, D. J. McGrail, N. D. Quach and M. R. Dawson, *Phys Biol*, 2014, 11, 056004.
22. N. Shoham, L. Mor-Yossef Moldovan, D. Benayahu and A. Gefen, *Tissue Eng. Part A*, 2015, 21, 1354-1363.
23. N. Shoham, P. Girshovitz, R. Katzungold, N. T. Shaked, D. Benayahu and A. Gefen, *Biophysical journal*, 2014, 106, 1421-1431.
24. P. N. Patel, C. K. Smith and C. W. Patrick, *Journal of Biomedical Materials Research Part A*, 2005, 73A, 313-319.
25. A. Gefen and E. Haberman, *J. Biomech. Eng.*, 2007, 129, 924-930.
26. S. Sen, A. J. Engler and D. E. Discher, *Cell Mol Bioeng*, 2009, 2, 39-48.
27. N. Ariotti, S. Murphy, N. A. Hamilton, L. Wu, K. Green, N. L. Schieber, P. Li, S. Martin and R. G. Parton, *Mol. Biol. Cell*, 2012, 23, 1826-1837.
28. J. R. Soine, C. A. Brand, J. Stricker, P. W. Oakes, M. L. Gardel and U. S. Schwarz, *PLoS Comput. Biol.*, 2015, 11, e1004076.
29. M. L. Rodriguez, B. T. Graham, L. M. Pabon, S. J. Han, C. E. Murry and N. J. Sniadecki, *J Biomech Eng-T Asme*, 2014, 136.
30. S. Schwarz Henriques, R. Sandmann, A. Strate and S. Koster, *J. Cell Sci.*, 2012, 125, 3914-3920.
31. C. Raupach, D. P. Zitterbart, C. T. Mierke, C. Metzner, F. A. Muller and B. Fabry, *Phys Rev E*, 2007, 76, 011918.
32. R. J. Pelham and Y. L. Wang, *Proc. Natl. Acad. Sci. U. S. A.*, 1997, 94, 13661-13665.